Pilot-Scale Lanthanide Precipitation from Sulfate-Based Spent Ni-MH Battery Leachates: Thermodynamic-Based Choice of Operating Conditions

Margot Zielinski, Laurent Cassayre, Nicolas Coppey, Béatrice Biscans

Pilot-Scale Lanthanide Precipitation from Sulfate-Based Spent Ni-MH Battery Leachates: Thermodynamic-Based Choice of Operating Conditions

Published as part of a Crystal Growth and Design virtual special issue in Celebration of the Career of Roger Davey

Margot Zielinski, Laurent Cassayre, Nicolas Coppey, and Béatrice Biscans*

ABSTRACT: Access to critical metals required for high-performance technologies, particularly, the light rare earth elements (REEs = La, Ce, Nd, Pr), has become a major challenge for import-dependent economies such as the European Union. In this regard, the recycling of spent nickel metal hydride (Ni-MH) batteries by hydrometallurgical processes can serve as an attractive secondary source of REEs. In such processes, precipitation of REEs from pregnant leach solutions (PLS) in sulfate media using Na_2SO_4 is often reported. However, little consideration is given as to whether and how sodium ions influence the precipitation efficiency and selectivity. This work focuses on a better understanding of the precipitation process by coupling pilot-scale (2 L) experiments on industrially sourced PLS containing 50 g/L of Ni and 17 g/L of REEs, with thermodynamic modeling, to assess the influence of temperature (25 °C < T < 60 °C) and the Na/REEs molar ratio (0.8:1 < Na/REEs < 3.2:1). Equilibria calculations were performed using OLI Systems Inc. software whose database covers rare earth sulfate compound properties and an accurate description of the aqueous electrolytes. Highly selective precipitation was obtained at 60 °C and for a Na/REEs molar ratio of 4:1. A lanthanide-alkali solid solution was identified by multianalytical characterization.

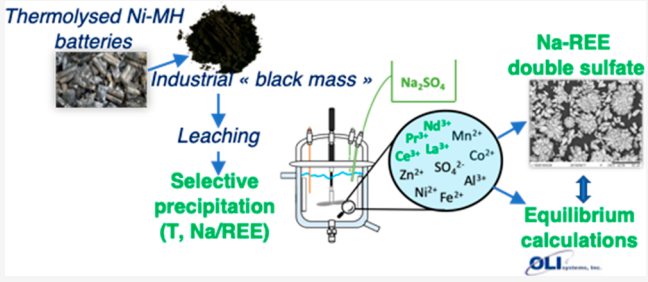

1. INTRODUCTION

Because of their unique physicochemical properties, rare earth elements (REEs) have become key constituents of high-performance technologies and energy storage materials—ranging from permanent magnets to electronic equipment, superconductors, polishing powders, pigments, and rechargeable battery electrodes, thus giving them undeniable worldwide economic importance.[1,2] Certain authors forecast an annual increase of the global demand for REEs of +8% from 2017 to 2025.[3] The term "rare" is a misnomer, the more abundant REEs such as lanthanum (La), cerium (Ce), neodymium (Nd), and praseodymium (Pr) being almost as concentrated in Earth's crust as more common metals such as Cu, Ni, or Co.[4] However, exploitable ore deposits are very dilute, and, consequently, REEs are only supplied from a few sources around the globe.[5] As of 2020, China dominates the REEs market and provides more than 86% of the global supply.[2]

High supply risks induced by this uneven distribution make light REEs some of the most critical metals, according to the European Commission's 2021 report on Critical Raw Materials.[2] Hence, it is crucial for highly import-dependent economies such as the European Union, to seek more locally sourced REE production. To this regard, spent nickel−metal hydride (Ni-MH) batteries can serve as an attractive secondary source of REEs. Indeed, the anode active mass of Ni-MH batteries is made of mischmetal where light REEs (La, Ce, Nd, and Pr) are alloyed with other metals (Ni, Co, Al, and Mn). The valuable powder extracted after crushing spent Ni-MH batteries can contain up to 15 wt % REEs.[6−9] Given that over a billion Ni-MH battery units have been placed on the market worldwide each year in the past decade[10] and that a compound annual growth rate (CAGR) of 2.6% for the global Ni-MH battery market is predicted between 2017 and 2022,[11] recycling of spent Ni-MH batteries has the potential to offer a significant feedstock for secondary REE production. However, because of technical (maturity of recycling

processes) and economic (volatility of raw materials prices) aspects, the contribution of recycling to the market demand is still very low. As of 2020, the end-of-life recycling input rate of La, Ce, Nd, and Pr are respectively <1%, <1%, <1%, and <10%.[2]

In the past decade, numerous academic and industrial research groups have focused on developing more efficient hydrometallurgical processes for the recovery of REEs from spent Ni-MH batteries. In a traditional process, spent batteries are transformed into a powder enriched in valuable elements thanks to thermal and mechanical pretreatment steps.[6,12] The powder is then leached in a mineral acid (HCl, HNO_3, or H_2SO_4) where REEs are solubilized in the pregnant leach solution (PLS) along with various other metal elements such as Ni, Co, Mn, Al, Fe, or Zn.[13] The bottleneck of the hydrometallurgical process is then to selectively separate these elements from each other. The type of mineral acid selected for leaching depends on the downstream separation process: generally, sulfuric media is chosen when precipitation is the preferred separation method, whereas hydrochloric or nitric systems are chosen when solvent extraction is preferred.[5] In this work, we have focused on selective precipitation as a recovery process. Elemental concentrations [g/L] obtained from a selection of the recent literature (2009−2021) having studied the leaching of spent Ni-MH battery powders in sulfuric media are summarized in Table 1. These data show rather wide concentration variations, which can be attributed to the leaching process parameters (solid−liquid ratio, leaching time). The leachates contain predominantly Ni (up to 50 g/L), while REEs represent roughly one-third of the Ni content.

A review of the literature shows that REEs can be precipitated in the form of oxalates or hydroxides by adding oxalic acid[20−22] or a base,[23] respectively, to the PLS. Under such conditions, however, the pH shift of REEs at around 6 is above that of other metals in solution (i.e., Fe, Al, Co, Ni, Mn, Zn), which does not yield good separation ratios. An alternative consists of precipitating REEs in the form of sparingly soluble monohydrated double sulfates $MREE(SO_4)_2 \cdot H_2O$ (M = K, Na; REE = La, Ce, Nd, or Pr) by the addition of Na^+ or K^+ ions according to the precipitation reaction (eq 1).[7,14,15,17,18]

$$REE^{3+}_{(aq)} + 2SO_4^{2-}{}_{(aq)} + M^+_{(aq)} + H_2O \rightarrow MREE(SO_4)_2 \cdot H_2O_{(s)} \quad (1)$$

The precipitation of sodium−lanthanide double sulfates is usually favored over that of potassium−lanthanide double sulfates since the solubility of the former is an order of magnitude lower than the latter, at room temperature.[24,25] In that case, the pH of the sulfate-based PLS is usually adjusted to 1.5−3.5 with a concentrated NaOH (3−10 M) solution[7,14,16,23,26,27] or a mixture of $NaOH/Na_2CO_3$[28,29] as it is believed that solely increasing the pH leads to the precipitation of REE double sulfates. Under optimal conditions, a highly selective precipitation of sodium-REE double sulfates with respect to other metals in solution is obtained.

In their recent experimental work, Porvali et al. demonstrated that the precipitation of REE double sulfates in sulfuric media does not depend so much on pH but rather on the Na^+ and SO_4^{2-} concentrations in solution.[15,17,19] Their strategy consists of extracting REEs by the addition of a Na_2SO_4 solution in order to increase Na/REEs and SO_4/REEs molar

Table 1. Typical PLS Elemental Concentrations [g/L] Obtained after Leaching Spent Ni-MH Batteries in H_2SO_4-H_2O Solvents

ref	[Ni]	[Al]	[Co]	[Fe]	[Mn]	[Zn]	[La]	[Ce]	[Nd]	[Pr]	total REEs
14	11.27	0.26	2.17	0.13	0.81	0.35	1.49	0.91	0.76		3.16
15	20.26		14.53	0.28	2.20		1.56	1.81	0.86	0.30	4.53
16	22.30		2.4	0.05	1.22	0.76	2.10	3.00	0.76	0.63	6.49
17	38.01		5.17	1.79			2.66	3.64		0.72	7.02
18	41.54	0.96	5.86	1.06	2.86	1.45	8.02				8.02
19	46.13	1.37	6.29	1.39	3.69	2.06	9.69	7.49		1.40	18.58
7	53.00		4.45	1.65	2.50	1.85	1.75	2.20	4.30	2.15	10.4
this work	52.3 ± 0.55	1.6 ± 0.02	4.6 ± 0.31	2.3 ± 0.32	3.1 ± 0.10	0.5 ± 0.02	11.2 ± 0.38	4.0 ± 0.23	1.3 ± 0.02	0.5 ± 0.01	17.0

ratios without necessarily increasing the pH value and, thus, preventing coprecipitation of other metals. The fact that the solubility of sodium-REE double sulfates decreases when the quantity of Na_2SO_4 in solution increases is linked to the common ion effect.[5]

In all of the studies regarding REE double sulfate precipitation from solutions obtained from leaching spent Ni-MH battery powders in sulfuric media, experimental results are very promising but are seldom correlated with thermodynamic equilibria calculations. Yet, thermodynamic simulations could help explain the observed precipitation mechanisms, optimize the conditions of REE extraction, and better design the recycling process. In the rare occasions where thermodynamic calculations are implemented, authors rely on models that do not take into account the complexity of the chemical system. For instance, some models do not represent the nonideality of the concentrated aqueous phase (and thus calculations are made for very diluted solutions).[1,19] Other models implement thermodynamic databases that cover the subsystem REE-(H_2SO_4)-H_2O (REE = La, Ce, Nd, or Pr) but do not consider the presence of sodium ions and therefore the possibility of precipitating sodium-REE double sulfates.[14]

Thermodynamic consideration of the more complex systems $REE_2(SO_4)_3$-Na_2SO_4-H_2SO_4-H_2O (REE = La, Ce, Nd, or Pr) has been made possible thanks to the recent (2019) modeling work of Das et al.[30] and the implementation of the corresponding thermodynamic data in the database of the OLI Systems Inc. software. One of the originalities of the present work, therefore, lies in the fact that we performed thermodynamic calculations representative of the experimental precipitation system using OLI Systems Inc. given the recent update of thermodynamic data relative to rare earth double sulfates. Thermodynamic equilibria were simulated for concentrated aqueous solutions consisting of spent battery leachates, over a wide range of temperature (25 °C < T < 60 °C) and added moles of Na_2SO_4 (0 mol < Na_2SO_4 < 0.32 mol). The modeling results were used as a guide for a parametric study to assess the influence of two main operating parameters on REE precipitation efficiency: temperature (25 °C < T < 60 °C) and final Na/REEs molar ratio (0.8:1 < Na/REEs < 3.2:1).

Precipitation experiments were carried out in a 2 L pilot-scale semibatch reactor, which constitutes another originality of this work compared to previous studies. Indeed, in the referenced literature, smaller reactor volumes of 100 mL,[19] 250 mL,[15] 500 mL,[7] or 1 L[14] are reported, which do not offer scalable precipitation conditions at industrial scale in terms of hydrodynamics and energy dissipation in the reactor. The objectives of the precipitation experiments reported in this article were to (i) better understand precipitation mechanisms at stake (precipitation kinetics, comparison with thermodynamic equilibria), and (ii) verify the truly selective nature of REE precipitation with respect to other metals when working with a PLS particularly concentrated in nickel ([Ni] ≈ 52 g/L) compared to most previous studies (Table 1). Furthermore, the crystals obtained in all precipitation experiments were characterized to investigate their structure, morphology, and purity.

2. MATERIALS AND METHODS

2.1. Pilot-Scale Setup of the Precipitation Experiments. Approximately 600 kg of cylindrical-type spent Ni-MH batteries were thermally deactivated, crushed, and sieved at the industrial facilities of SNAM (France) according to the protocol described in our previous work.[6] The black mass (BM) powder obtained after this thermomechanical treatment was prewashed in H_2SO_4-H_2O media at pH 6 to solubilize residues of alkali metals (Na, K) from the electrolyte and dried at 80 °C in an oven overnight. The prewashed BM powder was then leached in a 10 L semibatch reactor according to the procedure described elsewhere (H_2SO_4-H_2O, pH 1, 40 °C, solid−liquid ratio 15%).[13] After 27 h of leaching, insoluble residues were filtered out from the solution. A total of five leaching batches were carried out under the same conditions in order to provide a sufficient amount of leachate solution to perform precipitation experiments. For each precipitation experiment, 300 mL of solution from each leaching batch were mixed to obtain a total volume of approximately 1.5 L of initial solution. The mixed leachates used as initial solutions for the precipitation experiments were analyzed by inductively coupled plasma-optical emission spectroscopy (ICP-OES, PerkinElmer Optima 8300), and average elemental concentrations [g/L] are reported in Table 1.

Precipitation experiments were conducted in a 2 L jacketed semibatch baffled glass reactor equipped with a four-blade stirrer (Teflon, d = 7 cm in diameter). A total of 1.5 L of initial leachate solution was added into the reactor and regulated at a constant temperature (± 0.01 °C) using an ultracryostat instrument device (Thermo HAAKE circulator P2-CT50L). A constant mixing rate of 400 rpm was applied, ensuring sufficient mixing of the solution and a power dissipation in the reactor of approximately 6.9×10^{-1} W/m^3 of suspension.[31] The pH was carefully monitored ($\pm 10^{-4}$) using a pH sensor (Mettler Toledo probe). For all experiments, an aqueous precursor solution of Na_2SO_4-H_2O (Na_2SO_4 anhydrous powder, Sigma-Aldrich, >99.0% purity) was prepared at a fixed concentration of 2.87 M and maintained at 40 °C on a heating plate with magnetic stirring. To initiate the precipitation experiments, the precursor solution was added to the heated PLS at a constant flow rate of 7 g·min^{-1} in a simple jet, using a membrane pump (ProMinent) connected to the servo control system LabMax (Mettler Toledo).

The effect of two process parameters on REE precipitation was studied: precipitation temperature (T = 25, 40, and 60 °C, for a fixed final Na/REEs molar ratio of 3.2:1) and final Na/REEs molar ratio (0.8:1 < final Na:REEs molar ratio <3.2:1, at 60 °C). Na/REEs molar ratios are defined according to eq 2, in which $n(\mathrm{Na})\mathrm{added}_{V(Na_2SO_4,\,t)}$ is the number of moles of Na added in the reactor at time t (derived from the volume of precursor solution $V(Na_2SO_4)$ added in the reactor at time t), and $\sum n(\mathrm{La,Ce,Nd,Pr})_{t_0}$ is the sum of the moles of La, Ce, Nd, and Pr in the initial PLS.

$$(\mathrm{Na/REEs}) = \frac{n(\mathrm{Na})\mathrm{added}_{V(Na_2SO_4,\,t)}}{\sum n(\mathrm{La,\ Ce,\ Nd,\ Pr})_{t_0}} \quad (2)$$

Since for all the precipitation experiments, the same Na_2SO_4 precursor solution with the same Na_2SO_4 concentration was added at the same flow rate, Na/REEs molar ratios were increased by increasing the total addition time of Na_2SO_4. This implies an initial "semi-batch" period where the Na/REE molar ratio increases linearly as precursor solution is added, followed by a "batch" period where precipitation proceeds without further addition of the precursor solution, and the Na/REE molar ratio is fixed. Final Na/REEs molar ratios are calculated using (eq 2) considering the total added volume of precursor solution, corresponding to the end of the "semi-batch" period (t_0 is the initial time of the experiment).

The suspension was regularly sampled throughout the experiments (about 7 mL per sample) and filtered on 0.45 μm cellulose syringe filters. The elemental concentrations of the 10 following metals were determined by ICP-OES (PerkinElmer Optima 8300): Ni, Co, Mn, Fe, Al, Zn, La, Ce, Nd, and Pr. The experimental proportion of each element remaining in solution $P_{(i,t)\mathrm{exp}}$ [%] at sampling time t was calculated according to eq 3 where $C_{\mathrm{mas}}(i,t)$ is the mass concentration of element i in solution at sampling time t [mg/L], V_{sol,t_0} is the initial PLS volume [L], $V_{\mathrm{precursor},t}$ is the total volume of Na_2SO_4 solution added at sampling time t [L], $\sum V_{\mathrm{sample},t}$ is the accumulative volume of

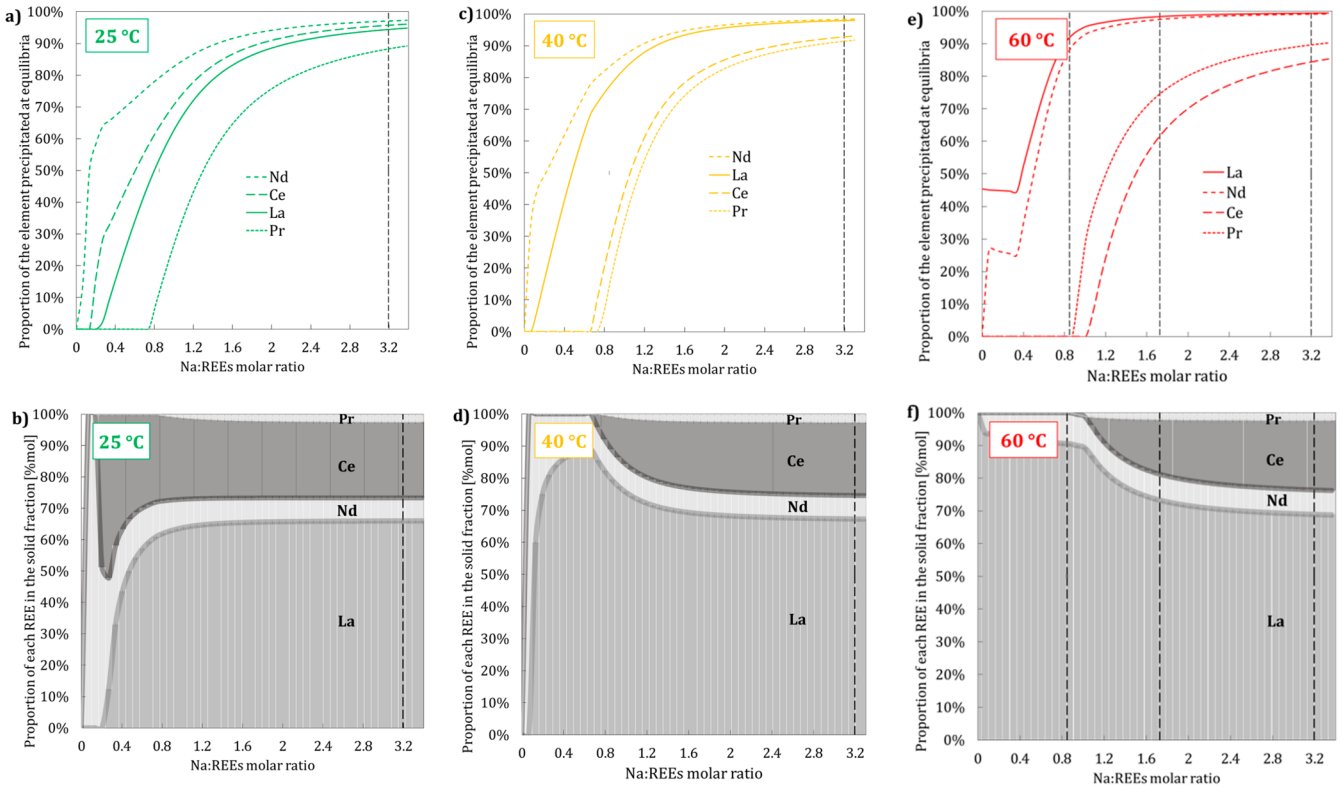

Figure 1. Proportion [%] of La, Nd, Ce, and Pr which should precipitate according to equilibria calculations at (a) 25 °C, (c) 40 °C and (e) 60 °C, and the proportion [% mol] of each REE in the solid fraction at (b) 25 °C, (d) 40 °C and (f) 60 °C (simulations performed with OLI Systems Inc.).

suspension extracted from the reactor at sampling time t [L] and $C_{mas}(i, t_0)$ is the mass concentration of element i in the initial PLS [mg/L]. Mass losses due to evaporation of the solution and/or gas generation were considered negligible.

$$P_{(i,t)\text{exp}} = 100*\frac{C_{mas}(i,\,t)*\left(V_{\text{sol},t_0} + V_{\text{precursor},t} - \sum V_{\text{sample},t}\right)}{C_{mas}(i,\,t_0)*V_{\text{sol},t_0}} \quad (3)$$

After 1 h, the suspension was filtered on a P3 borosilicate glass Büchner filter (4 L capacity), and the solid fraction was rinsed several times with demineralized water at room temperature. The obtained crystals (typically 65 g per experiment) were dried in an oven at 80 °C overnight before in-depth characterization using multiple techniques: scanning electron microscopy (SEM, JEOL JSM 7100F), laser diffraction (Malvern MS 3000), powder X-ray diffraction (XRD, D8 Bruker, 20° < 2θ < 80°, CuKα radiation, 1.5418 Å), thermogravimetric analysis (TGA, TA Instruments Q600, N_2(g), 25−600 °C, 5 °C/min, Pt crucible), microwave digestion (CEM MARS 6, 250 °C for 1 h in HCl/HNO_3 1:2, 1 g of powder in 30 mL), and ICP-OES (PerkinElmer Optima 8300, analysis of the 12 following elements: La, Ce, Nd, Pr, Na, S, Ni, Co, Mn, Al, Fe, Zn).

2.2. Thermodynamic Modeling. Thermodynamic equilibria calculations were used as a guide to delimit the studied range of operating conditions (temperature, final Na/REE molar ratios) and to compare theoretical concentrations in solution with experimental ones. Simulations were performed using the commercial software OLI Systems Inc., which implements the mixed-solvent electrolyte (MSE) model for concentrated electrolytic solutions[32] and features specifically the thermodynamic description of the systems $REE_2(SO_4)_3$-Na_2SO_4-H_2SO_4-H_2O (REE = La, Ce, Nd, or Pr).[30] This numerical tool allows the calculation of equilibria concentrations and speciation of the different species in an aqueous system, with respect to several parameters such as temperature and Na/REEs molar ratio. It is worth noting that the model only considers the possibility of forming a mixture of pure phases (i.e., REE-$Na(SO_4)_2$·H_2O with REE = La, Ce, Nd, or Pr) but does not consider the possibility of forming solid solutions (i.e., $La_wCe_xNd_yPr_zNa(SO_4)_2$·$H_2O$ with $w + x + y + z = 1$).

The metallic elements of the simulated PLS were introduced as sulfates either in the form of MSO_4 (M = Ni, Co, Mn, Fe, Al, or Zn) or $M_2(SO_4)_3$ (M = La, Ce, Nd, or Pr) in a volume of H_2O, in proportions corresponding to the experimental elemental concentrations in the PLS given in Table 1. A certain quantity of H_2SO_4 was also added to adjust the SO_4^{2-} total content of the experimental solution. Then, for a given temperature (25 °C < T < 60 °C), the simulation consisted of adding an increasing volume of the Na_2SO_4 solution to the initial PLS in order to simulate the experimental "semibatch" period, within a Na/REEs molar ratio range of 0:1−3.2:1. The output of the simulation provides the equilibrium proportion of each element which has precipitated $P_{(i,n(Na_2SO_4),T)\ \text{eq})}$ [%], as defined in eq 4, for a given temperature and a given amount of Na_2SO_4 added. The nature of the phases and the proportions of the elements in the solid fraction are also computed.

$$P_{(i,n(Na_2SO_4),T)\text{eq}} = 100*\left(1 - \frac{n(i)_{\text{liquid,eq}}}{n(i)_{\text{syst}}}\right) \quad (4)$$

where $n(i)_{\text{liquid,eq}}$ is the number of moles of element i in aqueous solution, and $n(i)_{\text{syst}}$ is the total number of moles of element i in the system at temperature T with respect to the Na/REEs molar ratio.

According to the definitions provided in eq 3 and in eq 4, $P_{(i,n(Na_2SO_4,T)\text{eq}}$ and $P_{(i,t)\text{exp}}$ are comparable quantities accounting respectively for the measured and calculated proportion of element i (Ni, Co, Mn, Fe, Al, Zn, La, Ce, Nd, Pr) having precipitated from the PLS.

3. RESULTS AND DISCUSSION

3.1. Thermodynamic-Based Choice of Operating Conditions. Results of the thermodynamic simulations indicate that within all operating conditions (25 °C < T < 60 °C; 0:1 < Na/REEs < 3.2:1) no metal element other than the REEs should precipitate, which proves the theoretical highly selective nature of this technique. The proportion of each REE which should precipitate (calculated according to eq 4) with respect to the Na/REEs molar ratio for different temperatures is plotted in Figure 1; the vertical dotted lines correspond to the final Na/REEs molar ratios selected for the experiments. When considering the sole impact of temperature without any addition of Na_2SO_4, all REEs are soluble at 25 and 40 °C (Figure 1a,c). However, at 60 °C, around 45% of La should precipitate, contrary to Nd, Pr, and Ce which remain soluble (Figure 1e). This corresponds to a precipitation of 30% of the REEs contained in the leachate. The model predicts that the solid phase which should form at 60 °C in the absence of Na_2SO_4 consists of an hydrated lanthanum sulfate $La_2(SO_4)_3 \cdot 9H_2O$ which precipitates according to eq 5. This corresponds to the fact that the solubility of $La_2(SO_4)_3 \cdot 9H_2O$ is regressive with increasing temperature[30] and that our PLS is close to La saturation.

$$2La^{3+}_{(aq)} + 3SO_4^{2-}{}_{(aq)} + 9H_2O \rightarrow La_2(SO_4)_3 \cdot 9H_2O_{(s)} \quad (5)$$

When the Na_2SO_4 solution is added to the leachate, the model indicates that, at 40 and 60 °C, Ce and Pr should not precipitate when the Na/REEs molar ratio is at least lower than 0.66:1 at 40 °C (Figure 1c) and at least lower than 0.87:1 at 60 °C (Figure 1e). On the other hand, at 40 °C and for a Na/REEs molar ratio of 0.66:1, 68% of La, and 78% of Nd should precipitate (Figure 1c); at 60 °C and for a Na/REEs molar ratio of 0.87:1, 93% of La, and 89% of Nd should precipitate (Figure 1e). It is worth to note that, under such conditions, the calculations suggest that a selective precipitation could be achieved, where La and Nd can be precipitated, whereas Ce and Pr remain in solution.

In the presence of Na_2SO_4, results of the thermodynamic calculations indicate that REEs form a monohydrated sodium-lanthanide double sulfate $REENa(SO_4)_2 \cdot H_2O$ (REE = La, Ce, Nd, or Pr), which precipitates according to eq 6 balanced out for 1 mol of Na_2SO_4.

$$2REE^{3+}_{(aq)} + 3SO_4^{2-}{}_{(aq)} + Na_2SO_{4(aq)} + H_2O \rightarrow 2REENa(SO_4)_2 \cdot H_2O_{(s)} \quad (6)$$

According to the simulations, the solid fraction obtained is therefore a mixture of pure REE double sulfates, where the relative molar contents of each REE [mol %] within the solid fraction can be determined according to eq 7. As can be seen in Figure 1d,f, at 40 and 60 °C for Na/REEs molar ratios of 0.66:1 and 0.87:1, respectively, the solid fraction is composed of 90 mol % La and 10 mol % Nd.

$$P_{solid,REE,n(Na_2SO_4),T} = 100 * \left(\frac{n(NaREE(SO_4)_2 \cdot H_2O)_{n(Na_2SO_4),T}}{\sum n(NaREE(SO_4)_2 \cdot H_2O)_{n(Na_2SO_4),T}} \right) \quad (7)$$

For Na/REEs molar ratios greater than 1:1, results indicate that the proportion of each REE which should precipitate increases with increasing Na/REEs molar ratios (Figure 1a,c,e). It is therefore preferable to work at elevated Na/REEs molar ratios in order to precipitate the majority of REEs: for instance, at 60 °C and for a Na/REEs molar ratio of 3.2:1, more than 95% of REEs should precipitate. It is interesting to note that the effect of temperature becomes negligible at sufficiently high Na/REEs molar ratios. Indeed, for a Na/REEs molar ratio of 3.2:1, the proportion of each REE in the solid fraction is relatively equivalent at 25, 40, and 60 °C; namely, the solid fraction consists of 67.3 ± 1.37 mol % La, 7.4 ± 0.09 % mol Nd, 22.9 ± 1.39 % mol Ce, and 2.4 ± 0.09 mol % Pr (Figure 1b,d,f). The relative proportions of REEs in the solid fraction are almost equivalent to the relative proportions of REEs in the initial PLS solution: 66.41% mol La, 7.35% mol Nd, 23.56 % mol Ce, and 2.68 % mol Pr.

In light of the above results, we carried out an experiment at 60 °C with a low final Na/REEs molar ratio of 0.8:1 to study the potentially selective precipitation of La and Nd with respect to Ce and Pr. Moreover, the overall objective being to extract a maximum of REEs during this precipitation step, we have also carried out experiments at 60 °C at higher final Na/REEs molar ratios of 1.7:1 and 3.2:1. Finally, experiments were carried out at 25 and 40 °C for a final Na/REEs molar ratio of 3.2:1 to investigate the influence of temperature on the kinetics of precipitation. Under such operating conditions, thermodynamic simulations suggest it is possible to extract more than 95% of REEs if equilibrium is reached and that identical proportions of REEs are expected in the solid fraction regardless of the temperature.

3.2. Precipitation Experiments. *3.2.1. Influence of the Final Na/REEs Molar Ratio.* The influence of the final Na/REEs molar ratio (0.8:1 < Na/REEs < 3.2:1) on REE precipitation was studied at a constant temperature of 60 °C. Throughout the experiments, pH evolution in the reactor was monitored, and results are described in Figure 2a. A simultaneous drop of pH is observed when the REE concentrations start to decrease (Figure 2a). With this observation, we show for the first time that pH monitoring can serve as an indicator of REE precipitation initiation. An induction period can thus be thus determined, which is about 3 min for all experiments carried out at 60 °C.

This sudden drop of the pH value could be explained by the displacement of the dissociation equilibrium of hydrogen sulfate HSO_4^- as described in eq 8.

$$HSO_4^- \leftrightarrow H^+ + SO_4^{2-} \quad (8)$$

Indeed, when REE double sulfates precipitate according to eq 6, 3 mol of sulfate ions SO_4^{2-} is consumed when 1 mol of Na_2SO_4 reacts. As a result, the dissociation equilibrium of hydrogen sulfate is likely to shift and liberate H^+ ions according to eq 8, which induces a drop in pH. On the opposite, when the solid's solubility limit is reached, the addition of Na_2SO_4 shifts the dissociation equilibrium toward HSO_4^-, which gradually increases the pH value.

Evolution of both the experimental and simulated concentrations [mol/L] of REEs with respect to time for different final Na/REEs molar ratios at 60 °C, are compared in Figure 3. The proportions of other metals (Al, Co, Fe, Mn, Ni, Zn) remaining in solution after 1 h of precipitation are given in Table SI.1. Overall, it can be seen that, experimentally, increasing the final Na/REEs molar ratio enhances the amount

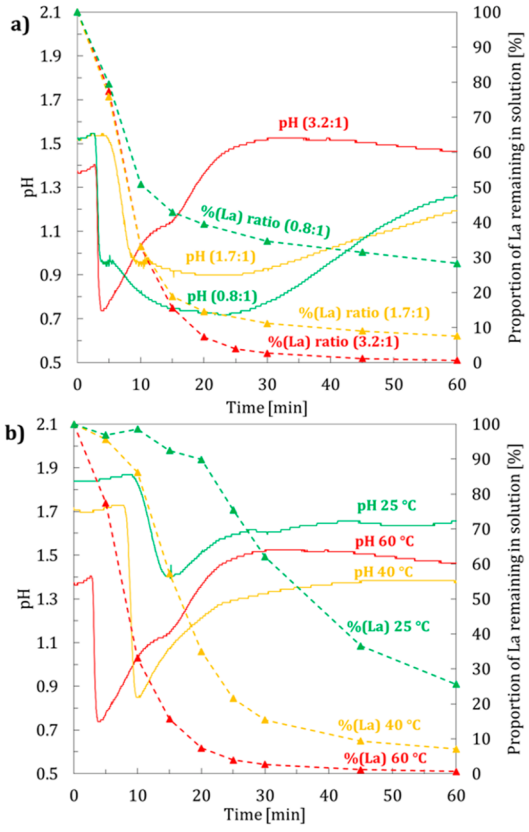

Figure 2. Evolution of pH, the proportion of La remaining in solution [%], and moles of Na_2SO_4 added with respect to time for the experiments carried out (a, c) at 60 °C and with final Na/REEs molar ratios of 0.8:1 (green), 1.7:1 (yellow), and 3.2:1 (red), and (b, d) at 25 °C (green), 40 °C (yellow), and 60 °C (red) for a fixed final Na/REEs molar ratio of 3:2:1.

of REEs which precipitate. Indeed, after 1 h of precipitation at 60 °C, a total of 73.4% REEs has been recovered for a final Na/REEs molar ratio of 0.8:1, 92.9% REEs for a ratio of 1.7:1, and 99.2% REEs for a ratio of 3.2:1. At 60 °C, it is not desirable to seek a further increase of the final Na/REEs molar ratio as nearly maximal REE precipitation efficiency is reached. Similar results have been obtained by Liu et al. (2019) who studied the precipitation of REE-Na double sulfates by the addition of Na_2SO_4 in a solution originating from sulfuric-based leaching of industrially treated spent Ni-MH batteries.[15] Their study shows that, after 1 h of precipitation at 70 °C, 74% of REEs precipitate for a 1:1 final Na/REE molar ratio, 88% for a 2:1 molar ratio, and 98% for 4:1 molar ratio. Moreover, our results show that at 60 °C and for a final Na/REEs molar ratio of 3.2:1, selective REE precipitation conditions are obtained since less than 5% of the other metals present in solution have precipitated (Table SI.1.).

As can be seen on Figure 3a,b, thermodynamic equilibrium is reached for La and Nd after 1 h of precipitation at 60 °C when the final Na/REEs molar ratio is 3:2:1. Indeed, experimental and thermodynamic concentrations of La are both 0.0005 mol/L, and those for Nd are 0.0000 and 0.0001 mol/L, respectively, which corresponds to the precipitation of 99.3% La and 99.7% Nd. On the other hand, for lower final Na/REEs molar ratios of 0.8:1 and 1.7:1, thermodynamic equilibria for La and Nd is not reached after 1 h of precipitation: only 71.7% La and 74.1% Nd have precipitated

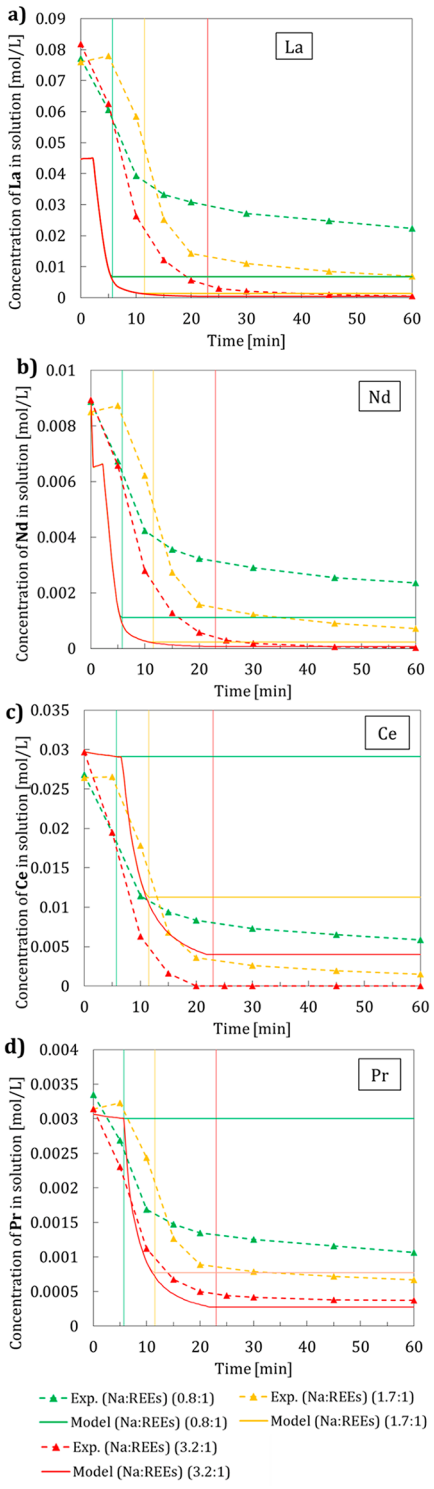

Figure 3. Evolution of the experimental (dotted lines) and simulated (full lines) concentrations [mol/L] of (a) La, (b) Nd, (c) Ce, and (d) Pr at 60 °C, for final Na/REEs molar ratios of 0.8:1 (green), 1.7:1 (yellow), and 3.2:1 (red). Vertical lines correspond to the end of the "semibatch" period. The equilibrium at time *t* is calculated for a system defined by the initial content of the reactor + amount of added Na_2SO_4 solution at time *t*.

experimentally for a molar ratio of 0.8:1, whereas simulations predict a precipitation of up to 90.9% La and 87.0% Nd. For a final Na/REEs molar ratio of (1.7:1), only 92.4% La and 93.5% Nd have precipitated experimentally, whereas simulations

predict up to 98.1% La and 97.2% Nd. This indicates slower precipitation kinetics when final Na/REEs molar ratios are decreased, and that for these lower ratios 1 h of precipitation is not enough to reach equilibria.

On the other hand, results indicate that more Ce precipitates experimentally than the quantities predicted by the model, at 60 °C and for all final Na/REEs molar ratios (Figure 3c). Similar observations can be drawn for Pr, particularly for a final Na/REEs molar ratio of 0.8:1 (Figure 3d). For instance, after 1 h of precipitation at 60 °C with a final Na/REEs molar ratio of 0.8:1, 79% Ce and 70% Pr have precipitated, whereas simulated thermodynamic equilibria suggest they should not precipitate.

Consequently, the predicted selective precipitation of La and Nd with respect to Ce and Pr at 60 °C for a final Na/REEs molar ratio of 0.8:1 was not achieved in our experiments. Similar results have been reported by Lister et al. (2021) who studied the recovery of Nd, Pr, and Dy contained in hard disk drives by leaching in HCl and precipitating REEs as double sulfates using Na_2SO_4.[5] The authors also used the OLI Systems Inc. software to simulate their experimental system, and in some cases observed significant recovery of some REEs, which was not predicted by the model.

The above discrepancies observed between experimental and thermodynamic concentrations of Ce and Pr in solution are most likely due to the formation of a solid solution, where Ce^{3+} and/or Pr^{3+} would be inserted or substituted within the crystal structure of $NaLa(SO_4)_2{\cdot}H_2O$ and/or $NaNd(SO_4)_2{\cdot}H_2O$. Theoretically, a solid solution could form given that the crystal structures of single phases of $NaREE(SO_4)_2{\cdot}H_2O$ (REE = La, Ce, Nd, or Pr) are all trigonal (space group $P_{3_2\,21}$ or the enantiomorphic analogue $P_{3_2\,21}$).[33−37] Moreover, the existence of solid solutions containing at least two REEs has previously been reported in the literature for other types of compounds such as rare earth oxides,[38] nitrates,[39] or phosphates.[40] Additionally, several authors have reported that stable solid solutions are favorable for adjacent lanthanide pairs (i.e., La−Ce, Ce−Pr, Pr−Nd) in nitrate[39] and phosphate[40] systems. In this case, the solid solution stabilizes the solid phase as opposed to a mixture of pure phases; therefore, a smaller amount of the element remains in solution when it has precipitated in the form of a solid solution than as a mixture of pure phases.[39]

As mentioned in section 2.2, the OLI system software does not allow taking into account the thermodynamic properties of solid solutions, which leads to overestimation of the quantities of Ce and Pr in solution. However, even if other software can make it possible to describe equilibria between solid solutions and concentrated aqueous solutions (e.g., Phreeqc, FactSage), there is to our knowledge no consistent thermodynamic description available for quaternary or higher-order systems REE-REE′-Na_2SO_4-H_2SO_4-H_2O (REE = La, Ce, Nd, or Pr). The main reason is that thermodynamic data regarding the solid mixtures has not yet been reported in the literature, and hence no model can account for the formation of a solid solution in our system of interest.

Solubility data regarding the quaternary or higher-order systems REE-REE′-Na_2SO_4-H_2SO_4-H_2O (REE = La, Ce, Nd, or Pr) have not yet been reported in the literature, and hence the model could not account for the formation of a solid solution and overestimated the quantities of Ce and Pr in solution. However, we can reasonably assume that solid solutions of $REE_xREE'_{1-x}(SO_4)_2{\cdot}H_2O$ are likely to form, particularly, solid solutions of the adjacent pairs $La_xCe_{1-x}(SO_4)_2{\cdot}H_2O$ and $NdxPr_{1-x}(SO_4)_2{\cdot}H_2O$.

From the solid side, it is interesting to represent the evolution of the relative molar contents [mol %] of REEs in the solid fraction with respect to time, or to the amount of Na_2SO_4 added, at 60 °C. The proportions obtained both with thermodynamic simulations (calculated according to (eq 7)) and with the experimental results (deduced from the difference between the initial amount of REE in the PLS and the amount in solution) are compared in Figure 4. According to the model,

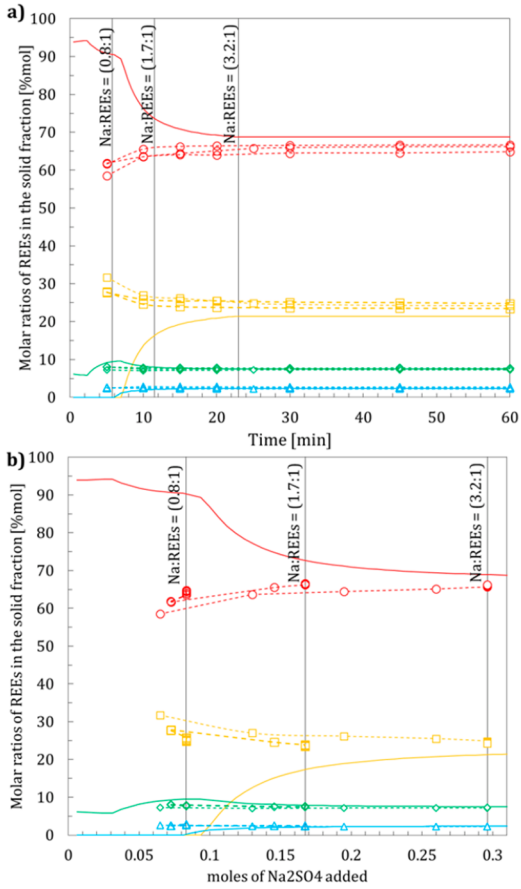

Figure 4. Comparison of the evolution of the molar ratios [% mol] of REEs in the solid fraction as obtained by thermodynamic simulations (continuous lines) and experiments (dotted lines) at 60 °C and for final Na/REEs molar ratios of 0.8:1, 1.7:1, and 3.2:1, with respect to (a) time and (b) the number of added moles of Na_2SO_4. The equilibrium at time t is calculated for a system defined by the initial content of the reactor + amount of added Na_2SO_4 solution at time t.

the relative molar contents of REEs in the solid fraction should differ significantly depending on the amount of Na_2SO_4 added (0 mol < $n(Na_2SO_4)$ < 0.32 mol). Experimentally, during approximately the first 10 min or during the addition of around 0.13 mol of Na_2SO_4 which corresponds to a Na/REEs molar ratio of 1.46:1, the composition of the solid fraction differs greatly from thermodynamic predictions, particularly in that it contains more Ce and less La than simulated. During this period, the experimental solid fraction is slightly enriched in La (58.5−61.8% mol to 63.5−65.5% mol) to the detriment of Ce (27.7−31.7% mol to 25.9−27.0% mol). After about 10 min, experimental curves flatten out, which indicates that at 60 °C

the composition of the precipitate does not depend on time or on the amount of Na_2SO_4 added (Figure 4). This observation at 60 °C suggests either (i) the formation of a mixture of pure phases of REE-Na double sulfates which maintain the same relative precipitation kinetics during the whole precipitation period or (ii) the formation of an identical single phase in the form of a solid solution. The average relative proportions of REEs in the solid fraction after 1 h are 65.6% mol La, 24.2% mol Ce, 7.5% mol Nd, and 2.5% mol Pr. The proportions of Nd and Pr in the solid fraction are nearly a perfect match to thermodynamic predictions (7.4% mol Nd and 2.4% mol Pr), whereas La and Ce contents are respectively lower and higher than thermodynamic predictions (67.3% mol La and 22.9% mol Ce). Consequently, our results demonstrate that, at 60 °C, the amount of Na_2SO_4 added or the choice of the final Na/REEs molar ratio has little influence on the composition of the solid fraction; however, increasing the final Na/REEs molar ratio leads to the extraction of a greater amount of REEs after 1 h (Figure 3).

Crystals obtained at the end of each experiment were characterized by various techniques. Size distributions were measured by laser diffraction and show very similar distributions with average mass diameters d_{43} in the 22.0–27.0 μm range. Size distributions are coherent with particle morphologies observed by SEM where agglomerates of several microns wide can be distinguished, of which elementary particles are composed of rhombohedra characteristic of the trigonal crystal structure (Figure 5). SEM analyses showed

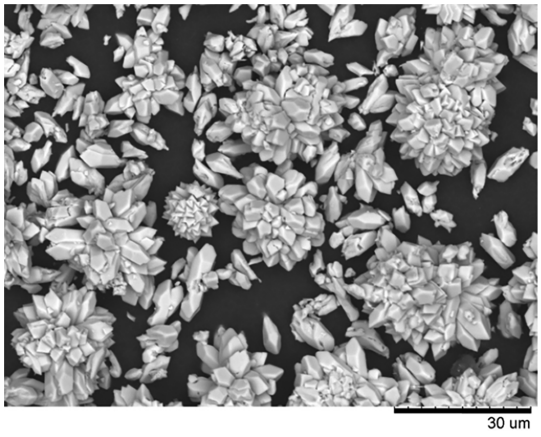

Figure 5. SEM micrograph of the crystals obtained after 1 h of precipitation at 60 °C and for a final Na/REEs molar ratio of 3.2:1.

similar crystal morphologies for all experiments. As can be seen in Figure 6a, powder XRD diffractograms of all the precipitates strictly overlap, which confirms that the same solid fraction is obtained as deduced previously from the analysis of the liquid fraction. Narrow peaks indicate precipitates are well crystallized, and the fact that there is no peak splitting strongly suggests the formation of one single phase in the form of a solid solution. The peaks have all been attributed to the pure phases $NaLa(SO_4)_2{\cdot}H_2O$ (PDF 01-086-0526) and $NaCe(SO_4)_2{\cdot}H_2O$ (PDF 01-082-1199), with slight deviations from the reference spectra (Figure 6a). No other crystalline phases can be identified. Our XRD results are in agreement with other works which have also precipitated REEs by adding either 3–10 M NaOH[7,14,16,23] or Na_2SO_4[17,18] to sulfate-based solutions originating from the leaching of spent Ni-MH batteries and

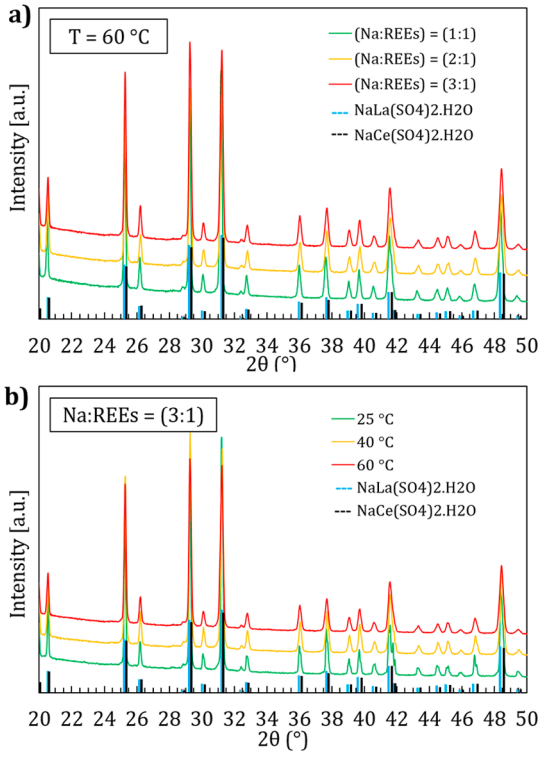

Figure 6. Powder XRD diffractograms of crystal obtained after 1 h of precipitation (a) at 60 °C and for final Na/REEs molar ratios of 0.8:1 (green), 1.7:1 (yellow), and 3.2:1 (red) and (b) at 25 °C (green), 40 °C (yellow), and 60 °C (red) for a final Na/REEs molar ratio of 3.2:1.

demonstrate thanks to XRD analyses that precipitates are chiefly composed of REE-Na double sulfates having a mixed crystal composition. However, no accurate chemical formula of the crystals has been reported so far.

The chemical compositions [wt %] of the precipitates determined after microwave digestion and ICP-OES analysis (La, Ce, Nd, Pr, Na, S, Ni, Co, Mn, Al, Fe, Zn) as well as TGA (determination of the water content) are detailed in Table 2. For the experiments carried out at 60 °C, very similar compositions are obtained regardless of the final Na/REEs molar ratio. Namely, precipitates contain on average 22.6 wt % La, 7.9 wt % Ce, 2.6 wt % Nd, and 0.6 wt % Pr. This corresponds to relative REE molar contents of 67.3% mol La, 23.3% mol Ce, 7.6% mol Nd, and 1.8% mol Pr, which is coherent with the relative contents deduced from the analysis of the liquid fraction (Figure 4). No traces of Co, Mn, Fe, and Zn were detected (below ICP-OES detection level); however, precipitates contain substantial amounts of Ni and Al, on average 5.7 wt % Ni and 1.8 wt % Al. Consequently, metal-based purities of 81.9 wt % on average are calculated according to eq 9 with wt %$_i$ being the relative weight contents [wt %] of metallic elements in the precipitates. Bertuol et al. (2009) obtained somewhat similar results after precipitating REE-Na double sulfates by adding 5 M NaOH to sulfate-based spent Ni-MH battery leachates, with a 91.93 wt % metal-based purity, 5.93 wt % Ni, and 1.16 wt % Co.[16]

$$\text{metal-based purity} = 100 - \frac{\text{wt \%}_{Ni} + \text{wt \%}_{Al}}{\text{wt \%}_{Ni} + \text{wt \%}_{Al} + \text{wt \%}_{La} + \text{wt \%}_{Ce} + \text{wt \%}_{Nd} + \text{wt \%}_{Pr}} \quad (9)$$

Table 2. Chemical Compositions [wt %] and Metal-Based Purities [wt %] of All the Obtained Precipitates

		chemical composition of the precipitates [wt %]									
temp [°C]	final Na/REEs molar ratio	SO_4	La	Ce	H_2O	Ni	Na	Nd	Al	Pr	purity [wt %]
60	(0.8:1)	48.72	22.47	7.71	5.35	5.84	4.91	2.61	1.79	0.60	81.0
60	(1.7:1)	48.91	22.69	8.02	5.31	5.19	4.99	2.69	1.61	0.59	83.3
60	(3.2:1)	48.41	22.56	7.94	5.45	6.03	4.55	2.60	1.86	0.61	81.4
40	(3.2:1)	48.45	22.36	7.80	5.29	5.65	5.44	2.66	1.75	0.61	81.9
25	(3.2:1)	48.73	21.37	7.81	5.75	5.70	5.55	2.68	1.76	0.65	81.3

The relatively significant impurity uptake observed in our results could be due to the coprecipitation of Ni and Al with REEs. Indeed, $Al(OH)_3$ and $Ni(OH)_2$ are known to have pH shifts around 4 and 6.5, respectively.[41] Locally high pH gradients in the reactor due to insufficient hydrodynamics could have led to the precipitation of the hydroxide phases. The fact that Ni- or Al-bearing phases were not detected by XRD could suggest that compounds are amorphous and thus not detectable by powder XRD; however, further characterization is required to confirm this hypothesis. If that is the case, crystal purities could be improved by washing the precipitates with hot water or a hot Na_2SO_4-H_2O solution rather than room temperature water because the solubility of $Al(OH)_3$ and $Ni(OH)_2$ increases with increasing temperature as opposed to that of REE-Na double sulfates.

3.2.2. Influence of Temperature. The influence of temperature (25 °C < T < 60 °C) on REE precipitation was studied for a fixed final Na/REE molar ratio of (3.2:1). The pH was monitored throughout the experiments, and results are detailed in Figure 2b. As previously mentioned, the simultaneous drop of pH when REE concentrations in solution start to decrease indicates that pH can serve as an indicator of the induction period. It is interesting to note that the induction period decreases with increasing temperature, namely, 10 min at 25 °C, 8 min at 40 °C, and 3 min at 60 °C. This observation is in agreement with the classical theory of 3D nucleation which stipulates that the induction period is inversely proportional to the logarithm of the supersaturation in solution.[42] Hence, with an increase of the temperature, the supersaturation in solution increases before the beginning of nucleation since the solubility of the REE-Na double sulfates decreases with increasing temperature.[30]

Experimental REE concentrations in solution with respect to time at different temperatures are compared with calculated equilibrium concentrations in Figure 7. Because the solubility of REE-Na double sulfates is regressive with temperature, increasing the temperature from 25 to 60 °C greatly increases precipitation efficiency of all REEs and yields faster precipitation kinetics. For example, after 1 h and for a fixed final Na/REEs molar ratio of 3.2:1, 77.6% of the REEs has precipitated at 25 °C, 94.5% at 40 °C, and 99.2% at 60 °C. Moreover, thermodynamic equilibria after 1 h of precipitation is reached only when working at an elevated temperature. After 1 h of precipitation at 25 °C, 74.4% La, 87.6% Ce, 77.5% Nd, and 69.3% Pr have precipitated experimentally, whereas the model predicts precipitation efficiencies of up to 94.4% La, 95.7% Ce, 97.1% Nd, and 88.3% Pr. At 40 °C, 92.9% La, 100.0% Ce, 94.4% Nd, and 84.3% Pr have precipitated experimentally after 1 h, whereas the model predicts precipitation efficiencies of up to 97.9% La, 92.7% Ce, 98.3% Nd, and 91.1% Pr.

Evolutions of the relative molar contents [mol %] of REEs in the solid fraction as deduced from the analysis of the liquid fraction from both the experiments and thermodynamic calculations are represented in Figure 8 with respect to the amount of Na_2SO_4 added and for different temperatures. When a total of 0.32 mol of Na_2SO_4 has been added, which corresponds to the final Na/REEs molar ratio of 3.2:1, the model predicts that the same solid fraction should form regardless of the temperature. This is verified by the experiments as the molar ratios are within close ranges for all temperatures: 63.4−66.3 mol % La, 24.2−27.0 mol % Ce, 7.2−7.3 mol % Nd, and 2.2−2.3 mol % Pr. However, although experimentally the same solid fraction appears to precipitate regardless of the amount of Na_2SO_4 added at 60 °C, this is not the case at 40 and 25 °C. Indeed, the experimental composition of the solid fraction with respect to the amount of Na_2SO_4 added evolves and more significantly so as the temperature decreases. This observation could indicate that, at 25 and 40 °C, (i) REEs precipitate in the form of a mixture of pure phases of REE-Na double phases, or (ii) the nature of the solid solution depends on both the temperature and the amount of Na_2SO_4 added. Further research is required on this aspect to determine which hypothesis prevails.

The filtered crystals obtained at different temperatures after 1 h of precipitation show very similar size distributions (22.8 μm < d_{43} < 26.1 μm) as indicated by laser diffraction and have precipitated as agglomerates of similar morphology as evidenced by SEM measurements. As represented in Figure 6b, peaks of the powder XRD diffractograms are thin and strictly overlap, suggesting the formation of a solid solution of constant composition for all temperatures after 1 h of precipitation. This observation is confirmed by the fact that crystals have nearly identical chemical compositions [wt %] and metal-based purities [wt %] (Table 2). They are composed on average of 22.1 wt % La, 7.9 wt % Ce, 2.6 wt % Nd, and 0.6 wt % Pr with metal-based purities of about 81.5 wt %.

4. CONCLUSION

A straightforward pilot-scale process was developed for the selective precipitation of REEs contained within a sulfate-based leachate originating from the industrial treatment of spent Ni-MH batteries.[13] The main objectives of this study were to (i) better understand the influence of operating parameters on precipitation mechanisms (precipitation kinetics, comparison with thermodynamic equilibria) and (ii) verify the truly selective nature of REE precipitation with respect to other metals when a concentrated Na_2SO_4 solution is added to a leachate particularly rich in Ni ([Ni] ≈ 52 g/L). One of the originalities of this work is that we performed equilibria calculations in the complex system MSO_4-$REE_2(SO_4)_3$-Na_2SO_4-H_2SO_4-H_2O (M = Ni, Fe, Co, Mn, Zn; REE = La, Ce, Nd, or Pr) with high initial concentrations of metal elements thanks to the OLI Systems Inc. software. This model benefits from the recent implementation of thermodynamic data related to REE sulfate compounds properties.[30]

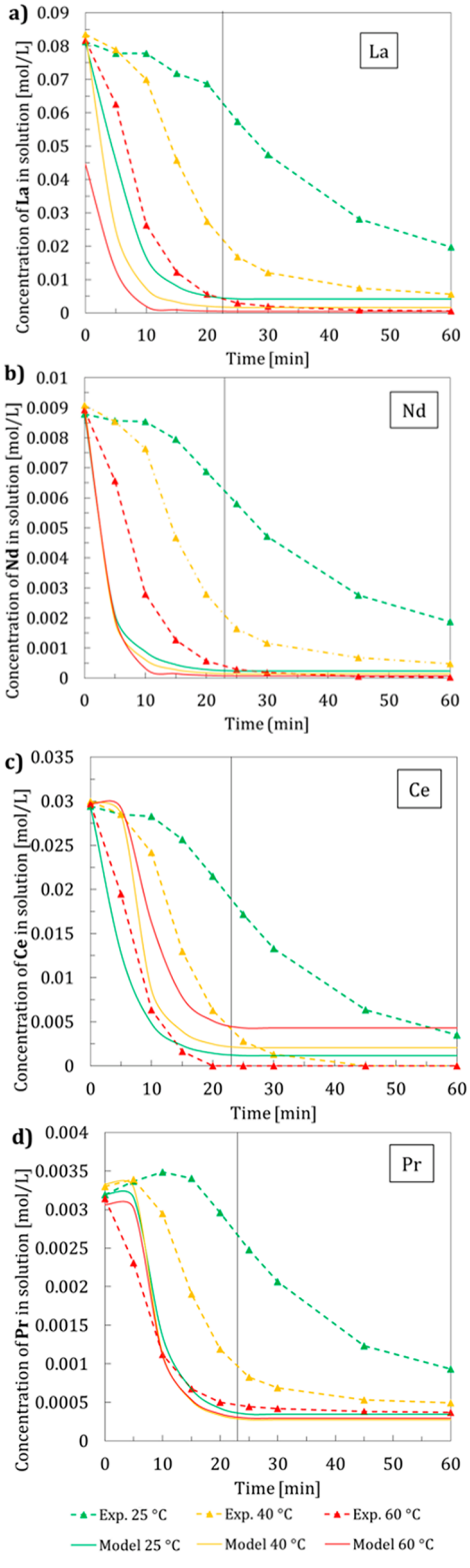

Figure 7. Evolution of the experimental (dotted lines) and simulated (full lines) concentrations [mol/L] of (a) La, (b) Nd, (c) Ce, and (d) Pr for a final Na/REEs molar ratio of 3.2:1 at 25 °C (green), 40 °C (yellow), and 60 °C (red). The vertical line corresponds to the end of the "semibatch" period. The equilibrium at time t is calculated for a system defined by the initial content of the reactor + amount of added Na_2SO_4 solution at time t.

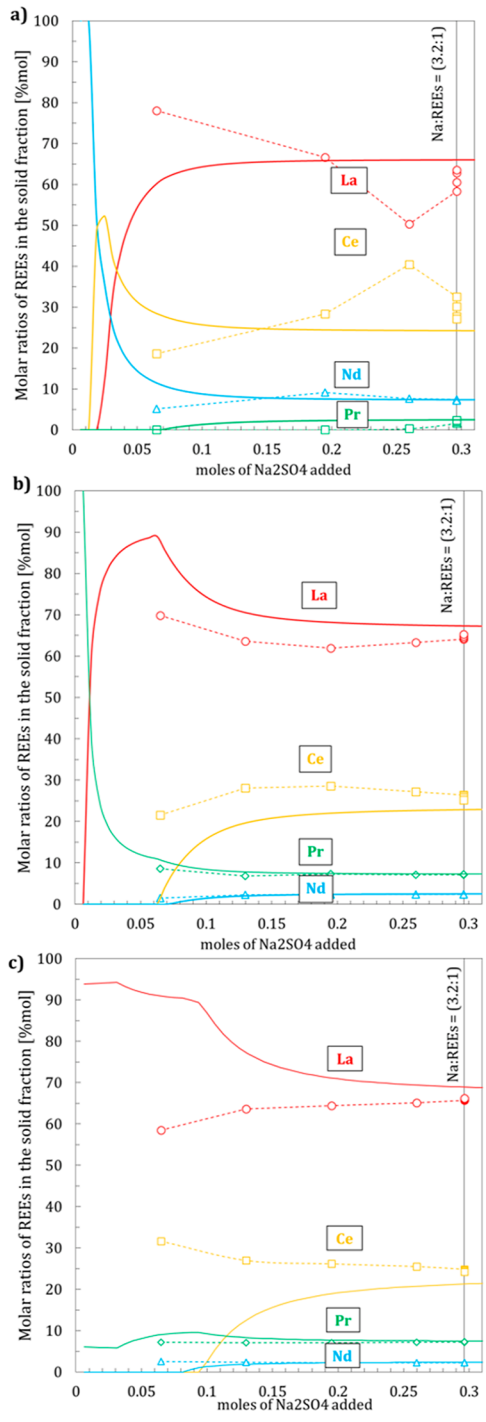

Figure 8. Comparison of the evolution of the molar ratios [mol %] of REEs in the solid fraction as obtained by thermodynamic simulations (continuous lines) and experiments (dotted lines) with respect to the number of added moles of Na_2SO_4 at (a) 25 °C, (b) 40 °C, and (c) 60 °C.

Simulations were used to guide an experimental parametric study to assess the influence of two operating parameters: temperature (25 °C < T < 60 °C) and final Na/REEs molar ratio (0.8:1 < Na/REEs < 3.2:1).

Modeling results indicate that the grouped selective precipitation of REEs is achievable because no other metal element than the REEs should precipitate and that a mixture of pure REE-Na double sulfates $REENa(SO_4)_2{\cdot}H_2O$ (REE = La,

Ce, Nd, or Pr) is expected. Results also demonstrate that increasing both temperature and final Na/REEs molar ratios should enhance REE precipitation efficiency because the solubility of the compounds decreases with increasing temperature and amount of Na_2SO_4 added. Furthermore, at a fixed temperature of 60 °C, the composition of the precipitated solid fraction is predicted to depend on the amount of added Na_2SO_4. On the contrary, thermodynamic predictions indicate that, for a fixed final Na/REEs molar ratio of 3.2:1, the composition of the precipitated solid fraction should not vary significantly between 25 and 60 °C.

Experimentally, the drop of pH observed when REE concentrations start to decrease showed for the first time that pH monitoring can serve as an indicator of REE precipitation initiation and allowed the determination of induction periods. Experiments carried out at 25 °C < T < 60 °C for a fixed final Na/REEs molar ratio of 3.2:1 were coherent with thermodynamic predictions: indeed, crystals obtained after 1 h of precipitation showed very similar chemical compositions regardless of the temperature. Experiments carried out at 60 °C and for 0.8:1 < final Na/REEs molar ratios < 3.2:1 were also in reasonable agreement with equilibria calculations; however, in some cases experimental results could not be reconciled with solubility calculations. Namely, results showed that at 60 °C the relative molar contents [mol %] of REEs in the solid fraction remained constant regardless of the amount of Na_2SO_4 added; in other words, increasing the amount of Na_2SO_4 added only enhances the quantity of REE extracted but does not modify the nature of the solid fraction as predicted by thermodynamics. This observation strongly suggests the formation of a single solid solution throughout the whole precipitation period at 60 °C in the form of $La_wCe_xNd_yPr_zNa(SO_4)_2{\cdot}H_2O$ ($w + x + y + z = 1$), which is backed by the absence of peak splitting in the XRD diffractograms of the crystals obtained after 1 h. Because of the current lack of solubility data regarding the systems REE-REE′-Na_2SO_4-H_2SO_4-H_2O (REE = La, Ce, Nd, or Pr), the model used it this study could not account for the formation of a solid solution and therefore in some cases overestimated the quantities of REEs in solution. Further work should include a more detailed structural characterization of the crystals to clarify the nature of the solid solution, as well as solubility studies to determine under which conditions REEs precipitate in the form of a mixture of pure salts or rather as a solid solution. Eventually, mixed double sulfate compounds could be added in the current thermodynamic database in order to improve the quality of the predictions.

Highly selective conditions were obtained after 1 h at 60 °C and for a final Na/REEs molar ratio of 3.2:1, whereby more than 99.2% of REEs precipitate, while more than 95% of the other metals (Ni, Co, Mn, Al, Fe, Zn) remain in solution. These precipitation conditions are totally transferable at the industrial scale leading to a more sustainable process with mild temperature (25 °C < T < 60 °C) and short batch time. Under such conditions, crystals contain 22.5 wt % La, 7.7 wt % Ce, 2.6 wt % Nd, and 0.6 wt % Pr with a metal-based purity of 81.0 wt %. The REE-free solution (70 ppm La, 0 ppm of Ce, 4 ppm of Nd, and 52 ppm Pr) is thus ready for further downstream processing to recover additional valuable metals such as Ni and Co.

■ ASSOCIATED CONTENT

Supporting Information

The Supporting Information is available free of charge at https://pubs.acs.org/doi/10.1021/acs.cgd.1c00834.

Proportion of metallic elements remaining in solution after 1 h of precipitation (PDF)

■ AUTHOR INFORMATION

Corresponding Author

Béatrice Biscans − *Laboratoire de Génie Chimique, Université de Toulouse, CNRS, INPT, UPS, Toulouse 31432, France;* orcid.org/0000-0002-2663-4357; Email: beatrice.biscans@toulouse-inp.fr

Authors

Margot Zielinski − *Laboratoire de Génie Chimique, Université de Toulouse, CNRS, INPT, UPS, Toulouse 31432, France; Société Nouvelle d'Affinage des Métaux (S.N.A.M.), Viviez 12110, France*

Laurent Cassayre − *Laboratoire de Génie Chimique, Université de Toulouse, CNRS, INPT, UPS, Toulouse 31432, France*

Nicolas Coppey − *Société Nouvelle d'Affinage des Métaux (S.N.A.M.), Viviez 12110, France*

Complete contact information is available at: https://pubs.acs.org/10.1021/acs.cgd.1c00834

Notes

The authors declare no competing financial interest.

■ ACKNOWLEDGMENTS

This research received financial support from the Agence Nationale de la Recherche et de la Technologie (ANRT) and La Région Occitanie (Project No. 19000678). The authors would like to thank Marie-Line de Solan-Bethmale from the Laboratoire de Génie Chimique (LGC) for the SEM analyses as well as Cédric Charvillat from the Centre Interuniversitaire de Recherche et d'Ingénierie des Matériaux (CIRIMAT) for the powder XRD measurements.

■ REFERENCES

(1) Kim, E.; Osseo-Asare, K. Aqueous stability of thorium and rare earth metals in monazite hydrometallurgy: Eh-pH diagrams for the systems Th-, Ce-, La-, Nd-(PO_4)-(SO_4)-H_2O at 25°C,. *Hydrometallurgy* **2012**, *113*−*114*, 67−78.

(2) Blengini, G. A. et al. *Study on the EU's List of Critical Raw Materials - Final Report*; European Commission, 2020.

(3) Leguérinel, M.; Lefebvre, G.; Christmann, P. *Séminaire COMES: Compétition entre secteurs industriels pour l'accès aux matières premières*, Mineralinfo, 2018.

(4) *Rare Earth Elements — Critical Resources for High Technology*; USGS, 2002.

(5) Lister, T. E.; Meagher, M.; Strauss, M. L.; Diaz, L. A.; Rollins, H. W.; Das, G.; Lencka, M. M.; Anderko, A.; Riman, R. E.; Navrotsky, A. Recovery of Rare Earth Elements from Recycled Hard Disk Drive Mixed Steel and Magnet Scrap,. *In Rare Metal Technology* **2021**, 139−154.

(6) Zielinski, M.; Cassayre, L.; Floquet, P.; Macouin, M.; Destrac, P.; Coppey, N.; Foulet, C.; Biscans, B. A multi-analytical methodology for the characterization of industrial samples of spent Ni-MH battery powders,. *Waste Manage.* **2020**, *118*, 677−687.

(7) Meshram, P.; Pandey, B. D.; Mankhand, T. R. Process optimization and kinetics for leaching of rare earth metals from the spent Ni-metal hydride batteries,. *Waste Manage.* **2016**, *51*, 196−203.

(8) Larsson, K.; Ekberg, C.; Ødegaard-Jensen, A. Dissolution and characterization of HEV NiMH batteries,. *Waste Manage.* **2013**, *33* (3), 689−698.
(9) Ebin, B.; Petranikova, M.; Ekberg, C. Physical separation, mechanical enrichment and recycling-oriented characterization of spent NiMH batteries,. *J. Mater. Cycles Waste Manage.* **2018**, *20*, 2018−2027.
(10) Pillot, C. The Rechargeable Battery Market and Main Trends 2016−2025. In *Advanced Automotive Battery Conference*; Cambridge Enertech, 2017.
(11) *Global Nickel-Metal Hydride (Ni-MH) Battery Market 2018−2022*; Technavio, 2018.
(12) Wang, H.; Friedrich, B. Development of a highly efficient hydrometallurgical recycling process for automotive Li-ion batteries,. *J. Sustain. Metall.* **2015**, *1*, 168−178.
(13) Zielinski, M.; Cassayre, L.; Destrac, P.; Coppey, N.; Garin, G.; Biscans, B. Leaching mechanisms of industrial powders of spent nickel metal hydride batteries in a pilot-scale reactor,. *ChemSusChem* **2020**, *13*, 616−628.
(14) Ahn, N. K.; Shim, H. W.; Kim, D. W.; Swain, B. Valorization of waste NiMH battery through recovery of critical rare earth metal: A simple recycling process for the circular economy. *Waste Manage.* **2020**, *104*, 254−261.
(15) Liu, F.; Peng, C.; Porvali, A.; Wang, Z.; Wilson, B.; Lundström, M. Synergistic recovery of valuable metals from spent NiMH and Li-ion batteries,. *ACS Sustainable Chem. Eng.* **2019**, *7*, 16103−16111.
(16) Bertuol, D. A.; Bernardes, A. M.; Tenorio, J. A. S. Spent NiMH batteries — The role of selective precipitation in the recovery of valuable metals,. *J. Power Sources* **2009**, *193*, 914−923.
(17) Porvali, A.; Wilson, B. P.; Lundström, M. Lanthanide-alkali double sulfate precipitation from strong sulfuric acid NiMH battery waste leachate,. *Waste Manage.* **2018**, *71*, 381−389.
(18) Porvali, A.; Agarwal, V.; Lundström, M. REE (III) recovery from spent NiMH batteries as REE double sulfates and their simultaneous hydrolysis and wet-oxidation,. *Waste Manage.* **2020**, *107*, 66−73.
(19) Porvali, A.; Ojanen, S.; Wilson, B. P.; Serna-Guerrero, R.; Lundström, M. Nickel Metal Hydride Battery Waste: Mechano-hydrometallurgical Experimental Study on Recycling Aspects,. *J. Sustain. Metall.* **2020**, *6* (1), 78−90.
(20) Pietrelli, L.; Bellomo, B.; Fontana, D.; Montereali, M. Characterization and leaching of NiCd and NiMH spent batteries for the recovery of metals,. *Waste Manage.* **2005**, *25* (2 SPEC. ISS), 221−226.
(21) Zhang, P.; Yokoyama, T.; Itabashi, O.; Wakui, Y.; Suzuki, T. M.; Inoue, K. Hydrometallurgical process for recovery of metal values from spent nickel-metal hydride batteries,. *Hydrometallurgy* **1998**, *50*, 61−75.
(22) Yang, X.; Zhang, J.; Fang, X. Rare earth element recycling from waste nickel-metal hydride batteries,. *J. Hazard. Mater.* **2014**, *279*, 384−388.
(23) Pietrelli, L.; Bellomo, B.; Fontana, D.; Montereali, M. R. Rare earths recovery from NiMH spent batteries,. *Hydrometallurgy* **2002**, *66*, 135−139.
(24) Lokshin, E. P.; Tareeva, O. A.; Ivlev, K. G.; Kashulina, T. G. Solubility of double alkali metal (Na, K) rare-earth (La, Ce) sulfates in sulfuric-phosphoric acid solutions at 20°C,. *Russ. J. Appl. Chem.* **2005**, *78* (7), 1058−1063.
(25) Lokshin, E. P.; Tareeva, O. A.; Kashulina, T. G. A Study of the Solubility of Yttrium, Praseodymium, Neodymium, and Gadolinium Sulfates in the Presence of Sodium and Potassium in Sulfuric-Phosphoric Acid Solutions at 20°C,. *Russ. J. Appl. Chem.* **2007**, *80* (8), 1275−1280.
(26) Innocenzi, V.; Vegliò, F. Recovery of rare earths and base metals from spent nickel-metal hydride batteries by sequential sulphuric acid leaching and selective precipitations,. *J. Power Sources* **2012**, *211*, 184−191.
(27) Rodrigues, L. E. O. C.; Mansur, M. B. Hydrometallurgical separation of rare earth elements, cobalt and nickel from spent nickel-metal-hydride batteries,. *J. Power Sources* **2010**, *195* (11), 3735−3741.
(28) Nan, J.; Han, D.; Yang, M.; Cui, M. Dismantling, Recovery, and Reuse of Spent Nickel-Metal Hydride Batteries,. *J. Electrochem. Soc.* **2006**, *153* (1), A101.
(29) Nan, J.; Han, D.; Yang, M.; Cui, M.; Hou, X. Recovery of metal values from a mixture of spent lithium-ion batteries and nickel-metal hydride batteries,. *Hydrometallurgy* **2006**, *84* (1−2), 75−80.
(30) Das, G.; Lencka, M. M.; Eslamimanesh, A.; Wang, P.; Anderko, A.; Riman, R. E.; Navrotsky, A. Rare earth sulfates in aqueous systems: Thermodynamic modeling of binary and multicomponent systems over wide concentration and temperature ranges,. *J. Chem. Thermodyn.* **2019**, *131*, 49−79.
(31) Zwietering, T. N. Suspending of solid particles in liquid by agitators,. *Chem. Eng. Sci.* **1958**, *8*, 244−253.
(32) Wang, P.; Anderko, A.; Young, R. D. A speciation-based model for mixed-solvent electrolyte systems,. *Fluid Phase Equilib.* **2002**, *203* (1−2), 141−176.
(33) Buyer, C.; Enseling, D.; Jüstel, T.; Schleid, T. Hydrothermal synthesis, crystal structure and spectroscopic properties of pure and Eu^{3+}-doped $NaY(SO_4)_2{\cdot}H_2O$ and its anhydrate $NaY(SO_4)_2$. *Crystals* **2021**, *11* (575), 575.
(34) Wickleder, M. S. Inorganic Lanthanide Compounds with Complex Anions,. *Chem. Rev.* **2002**, *102*, 2011−2087.
(35) Blackburn, A. C.; Gerkin, R. E. Sodium lanthanum(III) sulfate monohydrate, NaLa(SO4)2.H2O. *Acta Crystallogr., Sect. C: Cryst. Struct. Commun.* **1994**, *50* (6), 835−838.
(36) Blackburn, A. C.; Gerkin, R. E. Redetermination of sodium cerium(III) sulfate monohydrate, NaCe(SO4)2.H2O,. *Acta Crystallogr., Sect. C: Cryst. Struct. Commun.* **1995**, *51*, 2215−2218.
(37) Paul, A. K.; Kanagaraj, R. Synthesis, Characterization, and Crystal Structure Analysis of New Mixed Metal Sulfate NaPr(SO4)-2.H2O,. *J. Struct. Chem.* **2019**, *60* (3), 477−484.
(38) Han, X.; Wang, Y.; Hao, H.; Guo, R.; Hu, Y.; Jiang, W. Ce1-xLaxOy solid solution prepared from mixed rare earth chloride for soot oxidation,. *J. Rare Earths* **2016**, *34* (6), 590−596.
(39) Lassin, A.; Guignot, S.; Lach, A.; Christov, C.; Andre, L.; Made, B. Modeling the Solution Properties and Mineral - Solution Equilibria in Radionuclide-Bearing Aqueous Nitrate Systems: Application to Binary and Ternary Systems Containing U, Th, or Lanthanides at 25° C,. *J. Chem. Eng. Data* **2020**, *65*, 3613−3626.
(40) Carron, M. K.; Naeser, C. R.; Rose, H. J.; Hildebrand, F. A. *Fractional Precipitation of Rare Earths with Phosphoric Acid*; United States Government Printing Office: Washington, D.C., 1958.
(41) Monhemius, J. Precipitation diagrams for metal hydroxides, sulphides, arsenates and phosphates. *Trans. Institution Min. Metall.* **1977**, *86*, 202−206.
(42) Mullin, J. W. *Crystallization*, 3rd ed.; Butterworth-Heinemann: Oxford, 1993.